Proceedings of the Ninth Pacific Conference on Earthquake Engineering
Building an Earthquake-Resilient Society
14-16 April, 2011, Auckland, New Zealand

Preliminary source model of the M_W 7.1 Darfield earthquake from geological, geodetic and seismic data

C. Holden, J. Beavan, B. Fry, M. Reyners, J. Ristau, R. Van Dissen & P. Villamor

GNS Science, Lower Hutt, New Zealand

M. Quigley

Department of Geological Sciences, University of Canterbury, Christchurch, New Zealand

ABSTRACT: The M_W 7.1 Darfield earthquake has provided geologists, geodesists and seismologists with well constrained surface fault rupture extent and displacements, densely spaced GPS coseismic displacements, striking InSAR images, and a globally unprecedented set of near-source strong motion data. Collectively, these datasets indicate that the Darfield earthquake was a complex event, involving rupture of multiple fault planes with most of the earthquake's moment release resulting from dextral strike-slip movement on the previously unknown, east-west striking, Greendale Fault. They also point to important secondary sources such as a southeast-dipping blind reverse fault near Charing Cross that initiated the rupture sequence, and a northwest-dipping reverse fault near Hororata that increased rupture duration and spatial extent. Although the models are consistent and support each other, this analysis is still preliminary and ongoing research is focused on further integrating these data sets to better understand the nature, extent, depth and timing of sub-events of the Darfield earthquake.

1 INTRODUCTION

The M_W 7.1 Darfield earthquake occurred on Sept 4th 2010, approximately 40 km west of the city of Christchurch and ruptured a previously unmapped fault, the Greendale Fault (Fig. 1). The earthquake had a small impact on modern buildings but caused extensive liquefaction and damage to earthquake-risk buildings (Cousins *et al*. 2010, Van Dissen *et al*. 2011, Zhao and Uma 2011).

The earthquake was a unique event; It was the first major "internet age" quake for New Zealand, provided a very large amount of data, ruptured on a superbly defined fault trace, and caused no casualties despite extreme recorded ground motions.

Early on, two seismological observations suggested that this earthquake was a complex event (Gledhill *et al*. 2010, 2011). The epicentre was located off the trace of the surface fault rupture (presumably steeply-dipping), and the focal mechanism solution is non-unique: the teleseismic moment tensor solution indicates a strike-slip mechanism, but the regional moment tensor solution and first-motion polarities indicate a reverse mechanism. The complexity of the rupture is also reflected in the extensive high-quality geological, geodetic and strong motion datasets, as described below.

In this paper we present fault-rupture models for the 4th September earthquake. Models are obtained from geological, geodetic, and seismological datasets. Although still preliminary, our results show a consistent model of a complex fault rupture.

2 SOURCE MODEL CONSTRAINTS FROM GEOLOGICAL DATA

2.1 Geological mapping of surface fault rupture

Scientists from the University of Canterbury responded to the earthquake immediately and within five hours had identified a surface fault rupture. GNS scientists also mobilised and joined the field team on the day of the earthquake. Initial mapping involved visual observations from land as well as by helicopter. Over the next few weeks, a detailed map of surface rupture along the previously unrecognised Greendale Fault (with a resolution of less than 10 cm) started to take shape (Fig. 1), based on measurements derived from tape and compass, differential and Real Time Kinematic (RTK) GPS surveys, terrestrial laser scanning, aerial photography, and airborne Light Detection And Ranging (LiDAR). The flat and intensely farmed agricultural landscape provided a wealth of markers from which to measure offsets (e.g. roads, fences, irrigation channels, and power lines).

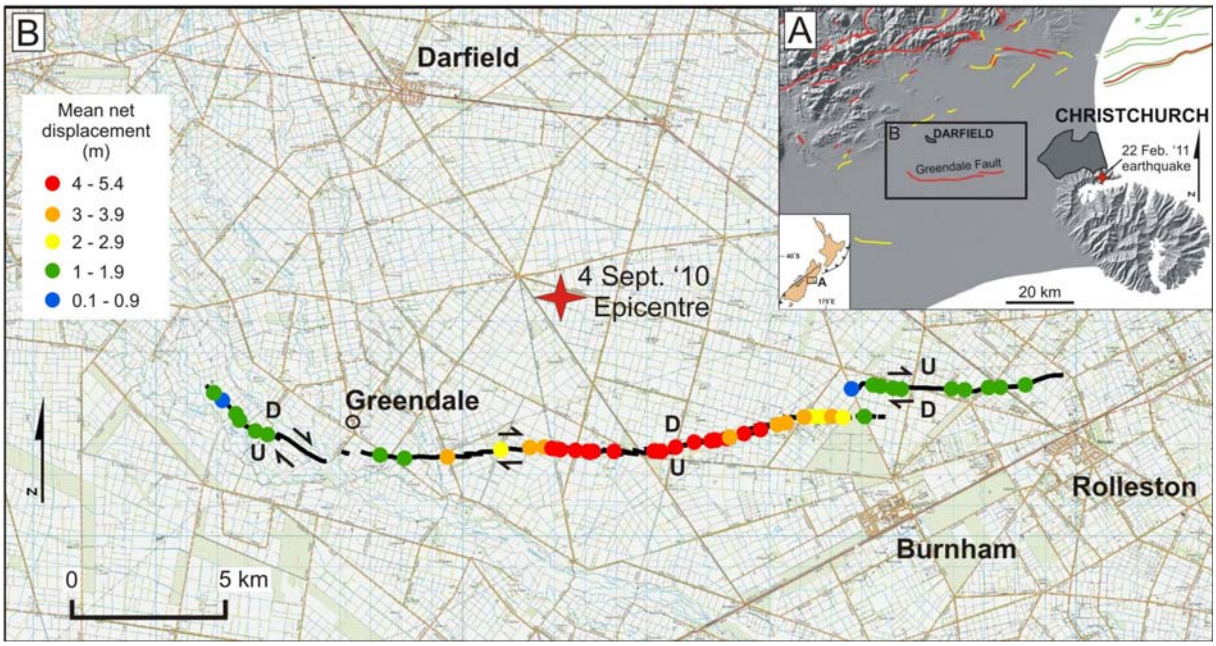

Figure 1. A) Digital Elevation Model (DEM) of the Christchurch area of the Canterbury region showing location of the Greendale Fault and other tectonically active structures. Red lines are active faults, and yellow and green lines are, respectively, on-land and off-shore active folds (combined data from Forsyth *et al*. (2008) and GNS Active Faults Database, http://data.gns.cri.nz/af/). B) Mapped surface trace (black line) and measured surface rupture displacements (coloured dots) along the Greendale Fault (Quigley *et al*. 2010). Black arrows indicate relative sense of lateral displacement, while vertical displacement is denoted by black U = up and D = down. Red four-pointed star in B is Darfield earthquake epicentre (Gledhill *et al*. 2010, 2011), and inset A shows epicentre of the smaller, but much more tragic, M_w 6.2, 22 February, 2011, aftershock event.

A major feature of the surface fault rupture was the large dextral displacements. The maximum displacement was 5 m in the central portion of the fault, and the average displacement was 2.5 m over the whole fault trace length of 29.5 km. Maximum vertical displacement was ~1.5m, but generally < 0.75m. The rupture is mostly east-west striking but has a northwest striking segment west of the hamlet of Greendale (Fig. 1). The southern side of the fault trace is upthrown everywhere, except for the eastern fault segment, near Rolleston, where the northern side is upthrown.

2.2 Source model from geological observations

The geological evidence would suggest the fault is generally steeply dipping. The NW Greendale segment appears to have a normal component, and therefore the fault most likely dips north. The large displacements and varying rupture characteristics long the Greendale Fault trace are suggestive of a complex rupture process for the Darfield earthquake. The Greendale Fault surface rupture has an unusually large amount of slip for its length in comparison with worldwide datasets of historic surface ruptures (e.g. Wesnousky 2008, Wells & Coppersmith 1994). Also, according to simple scaling relationships proposed by the above two papers, the rupture length should indicate a M_w 6.8 rather than M_w 7.1. The estimated magnitude increases slightly to M_w 6.9 when applying a recently developed regression for low slip-rate reverse and strike-slip New Zealand earthquakes (Stirling *et al*. 2008, Quigley *et al*. 2010). The mapped length of surface fault rupture associated with the Darfield earthquake along the Greendale Fault suggests that rupture of this fault accounted for the main seismic moment release of the earthquake. However, it does not account for the total seismic moment released.

3 SOURCE MODEL FROM GEODETIC DATA

3.1 Geodetic and InSAR data acquisition

Eighty previously-surveyed GPS sites within 80 km of the epicentre were measured in the week following the earthquake to include as little post seismic slip as possible. (Fig.2). A number of synthetic aperture radar images (InSAR) were obtained using ALOS/PALSAR data from the Japanese Space Agency and Envisat data from the European Space Agency (Beavan *et al*. 2010). These radar images were processed to acquire differential interferometric synthetic aperture radar (DInSAR) images showing ground deformation in the line of sight from the ground to the satellite (Figure 3).

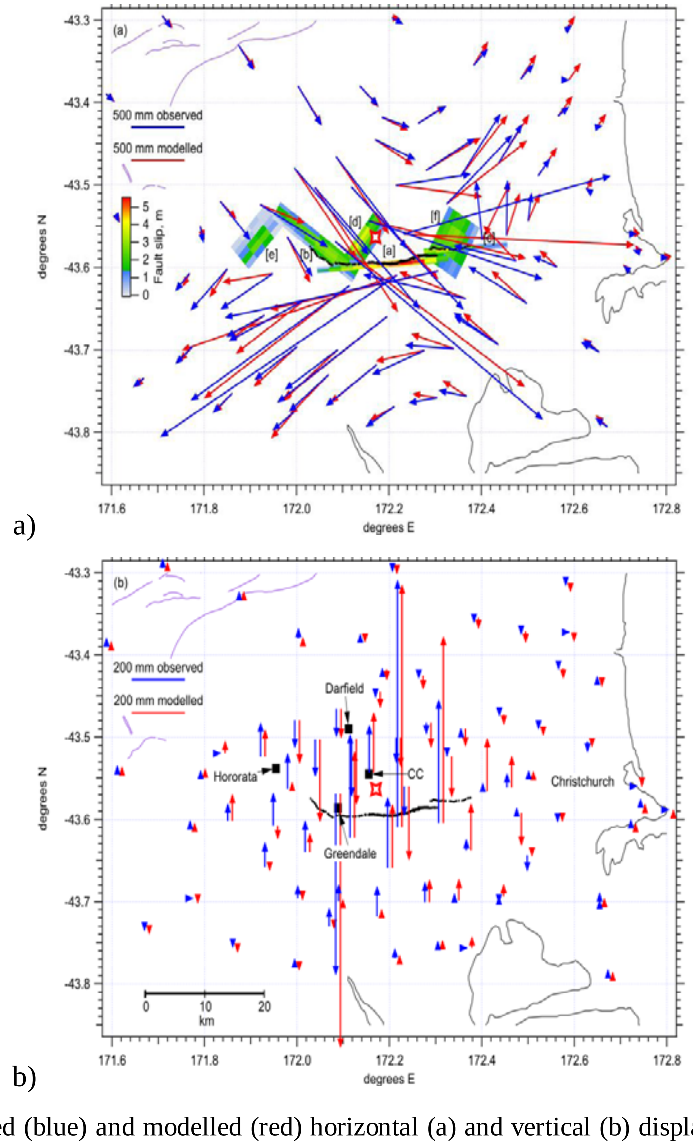

Figure 2. GPS observed (blue) and modelled (red) horizontal (a) and vertical (b) displacements. Red and white four-pointed star shows the epicentre. Black line shows the mapped surface rupture of the Greendale Fault. The coloured image in (a) shows the projection to the Earth's surface of the preliminary distributed slip model. The

model consists of slip on the Greendale Fault plus three thrust segments on NE-oriented planes. Place names referred to in the text are indicated by filled black squares in (b); CC is Charing Cross.

Maximum displacements of nearly 2 m in the horizontal direction and 1.5 m vertically were observed in the epicentral area (Fig. 2). The InSAR data (Fig. 3) shows some fringe discontinuities near the epicentre, as well as an isolated fringe pattern on the western side of the fault rupture.

3.2 A preliminary static 3D source model

The data inversion involves a 2 step method: firstly only the GPS data are inverted to search for fault plane locations and geometries with uniform slip distribution; secondly both GPS and InSAR data are inverted to search for a variable slip distribution and rupture mechanism, and also to refine the fault-plane geometries. The proposed model is described on Figure 2 (projected slip at the surface) and Figure 4 (3D views of the fault planes). It consists of a segmented Greendale Fault plane and three additional blind faults.

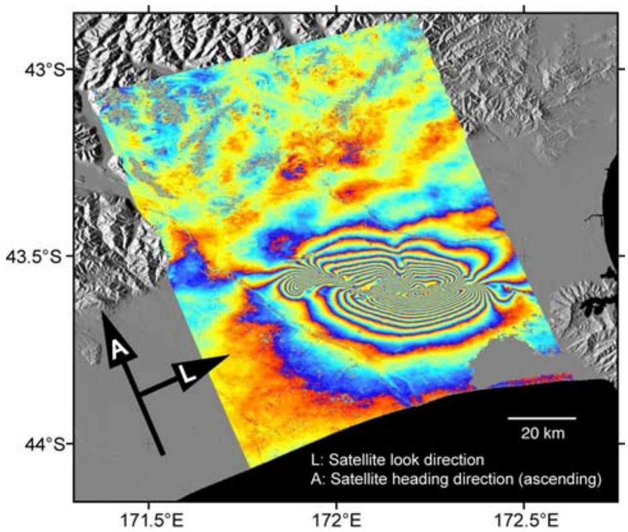

Figure 3. Original ALOS interferogram showing interference fringes that each represent 118 mm of ground motion in the line-of-sight to the satellite. The east-west and northwest-southeast strands of the Greendale Fault are clear in this image, as are the signatures of blind thrust faults near Charing Cross and Hororata. For the outer parts of the image it is clear that it is easy to unwrap the fringes to obtain the total ground displacement relative to the far field. This becomes progressively harder as the fringes get closer together (i.e., the displacement gradient increases) and as the coherence becomes lower. Regions of low coherence are concentrated along the Greendale Fault surface rupture and near the up-dip (northwest) end of the Charing Cross blind reverse fault on which the initial rupture occurred.

The Greendale Fault plane is characterized by an east-west striking central segment, taking up most of the moment release, and equivalent to a M_w 6.9 earthquake (note 4.5 m of dextral displacement at the surface is consistent with geological observations), an east-west striking segment to the east corresponding to M_w 6.6, and a NW-SE striking segment to the west, equivalent to M_w 6.6.

The three blind fault rupture planes have a reverse displacement component. The "Charing Cross" fault (equivalent to M_w 6.5) is located between Greendale and Charing Cross, and it is consistent with the seismological observations of the location of the initiation of the Darfield earthquake. A fault near Hororata, (equivalent to M_w 6.2) is consistent with observations of ground displacements from the InSAR data and superficial ground cracks in the area (Quigley *et al.*, 2010). Finally a poorly-constrained fault (equivalent to M_w 6.5) is located near the step-over of the Greendale Fault. More details on the fault rupture parameters can be found in Beavan *et al.* (2010).

The geodetic model was built upon and supports the geological model. Major features such as maximum slip amplitude and locations, and fault segment orientations, are consistent. The complexities in the geodetic model are where the geology sees changes of rupture pattern (bend west of Greendale, step-over near Rolleston). The geodetic model brought more details into the rupture pattern, highlighting the presence of blind reverse faults of significant magnitude. The overall moment release for this model is equivalent to M_w 7.0.

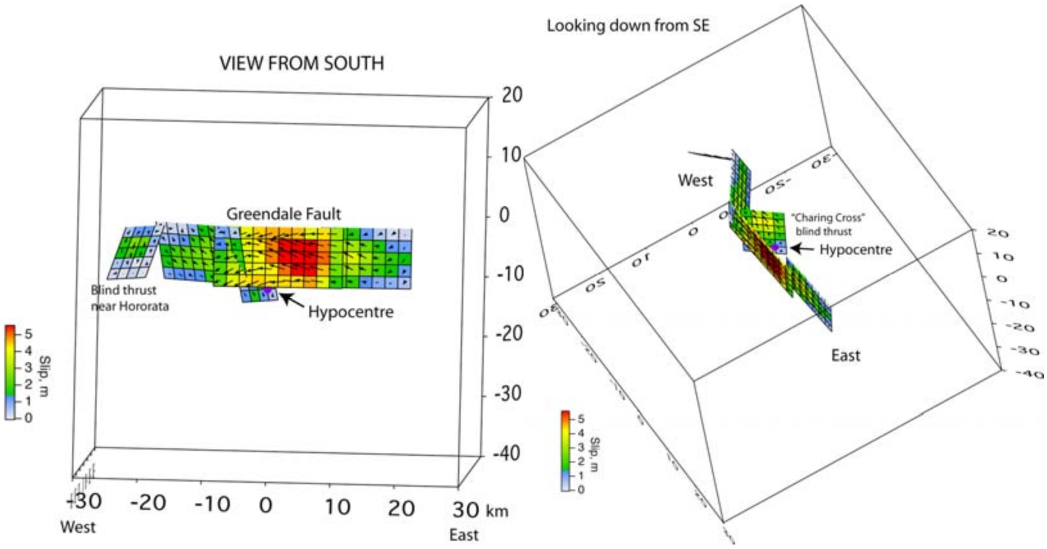

Figure 4. Inferred slip distribution on the geodetic model fault surfaces. The arrows show slip vectors of the hanging wall relative to the footwall. The coloured image gives the slip magnitude. The Greendale Fault is modelled as three separate segments. The geographic locations of the fault segments are indicated on Figure 2a.

4 SOURCE MODEL FROM SEISMIC DATA

4.1 The strong motion dataset

We inverted 3-component seismograms from 17 stations well-distributed around the epicentre and closer than 35 km (Fig. 5). Seismograms were integrated into velocities and band pass filtered up to 0.2 Hz. We invert for variable slip amplitude and direction, as well as for rupture-time history on fixed fault planes (Di Carli *et al*. 2010). We inverted data for a source on the Greendale Fault plane, first on a straight east-west striking plane. Then we added the northwest striking western segment based on the geological mapping. Residuals on the waveform-fits near the epicentre, as well as the regional moment tensor solution, both suggested that another fault plane with a reverse faulting mechanism was involved. Therefore, we added the "Charing Cross" Fault plane in our inversion. Finally, we added a third fault plane near Hororata based on (i) large waveform fit residuals near Hororata station (HORC) from a concentration of large aftershocks in this area, and (ii) a strong signal from the InSAR data suggesting the presence of a third fault plane to the west of the Greendale Fault. Our preliminary seismological fault-geometry model consists of three fault surfaces, the Greendale Fault surface, the Charing Cross Fault plane and the fault plane near Hororata (Fig. 5 and 6).

4.2 A preliminary 3D kinematic source model

The kinematic fault model to be described below (Fig. 6) provided very good waveform fit between observed and synthetic seismograms, matching the large amplitude of the signals as well as arrival phases. Figure 7 shows the waveform fit between observed data (black), synthetic data from a single Greendale Fault model (blue) and synthetic data from a proposed 3-fault model (red). The addition of a blind reverse source at the epicentre improves the fit for the first few seconds of the signals, especially for the Darfield (DFHS) and Greendale (GDLC) stations. The addition of the reverse fault plane near Hororata helps with matching the second large peak observed at HORC after 18 seconds, as well as later phases on GDLC, for example.

Our preliminary rupture history for the Darfield event is as follows. The rupture started on the steeply-dipping Charing Cross blind reverse fault, and ruptured between 3 and 6 seconds (we are not able to resolve for the very small initial amplitudes yet). The maximum slip was 3.7 m at 6.5 km depth, and almost purely reverse faulting (102º rake on the fault plane). This initial sub-event was equivalent to a magnitude Mw 6.2 earthquake.

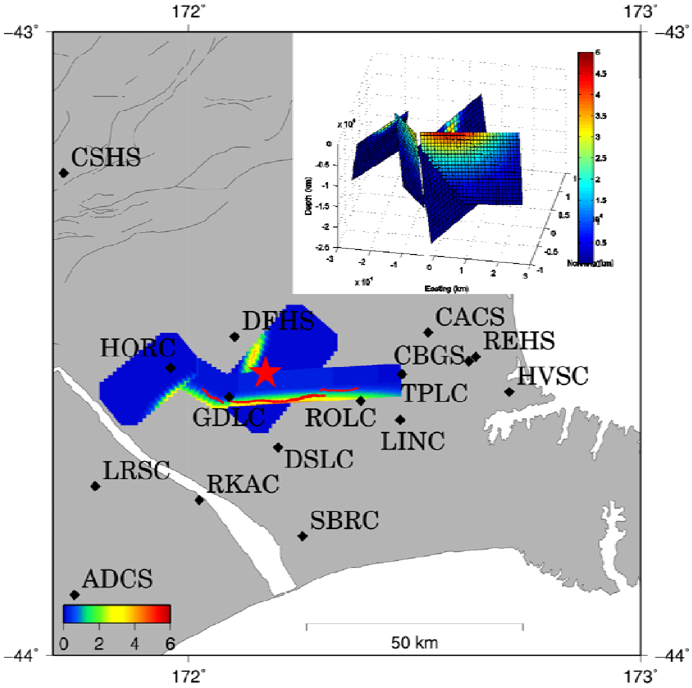

Figure 5. Map showing the surface projection of the slip distribution from the 3D seismological fault rupture model, the strong motion stations, the mapped surface trace (red) and the Darfield epicentre (red star); top right corner: 3D rupture model showing the Greendale Fault plane with the east-west and north striking segments, the reverse fault plane near Hororata to the west, and the Charing-Cross reverse fault near the epicentre.

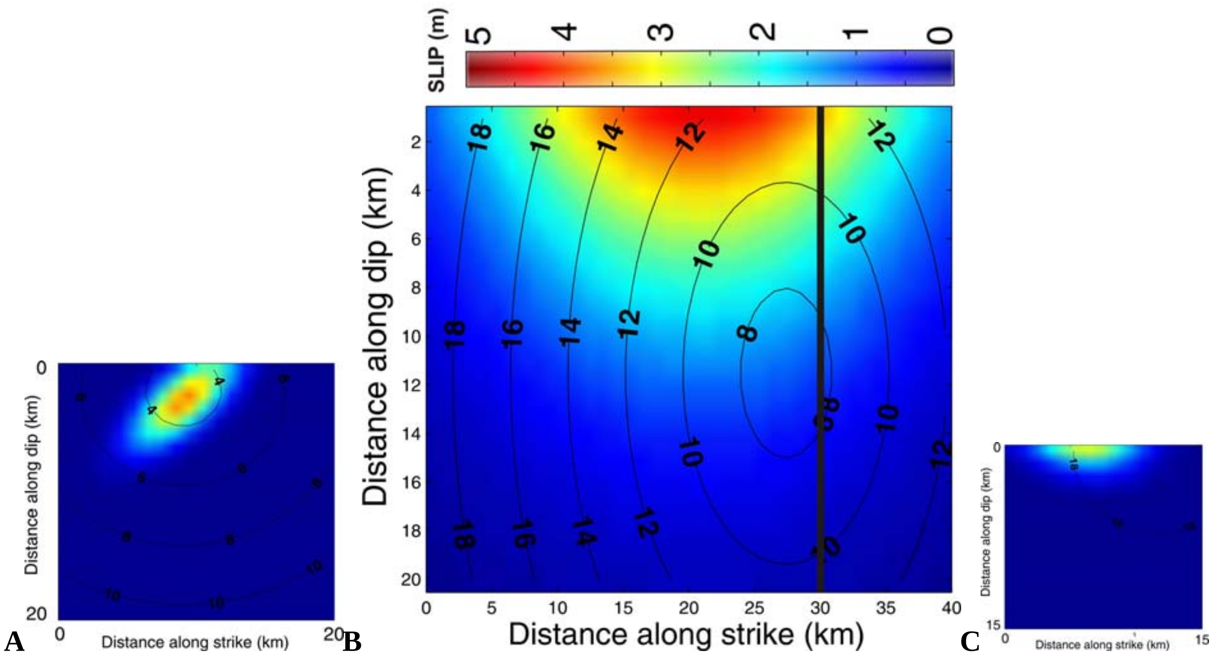

Figure 6. Fault segments and rupture time contour history for the kinematic model inferred from the strong motion data. The plots are scaled to reflect the relative contribution (overall fault size) of each fault plane. A is the Charing-Cross reverse fault near the epicentre, where the rupture initiated (looking perpendicular to the fault strike, towards the northwest); B is the Greendale Fault plane, looking towards the south, where the rupture initiated at depth and ruptured towards the west and mostly towards Christchurch between 8 and 18 seconds; the

vertical black lines separates the east-west striking segment (left) from the northwest bending one (right) near the hamlet of Greendale; C is the fault plane near Hororata where the rupture occurred after 17 seconds and near the surface (looking perpendicular to the fault strike, towards the east).

Rupture then occurred along the Greendale Fault plane in a bilateral mode for about 10 seconds, between 8 and 18 seconds, reaching a maximum displacement of 5 m at the surface. The rupture directivity was strongly towards Christchurch. The slip rake is mostly right lateral with a slight normal component. This is equivalent to a magnitude M_w 6.8 event, making it the largest of the three events.

After 17 seconds, the fault near Hororata ruptured, reaching a maximum slip of 2.8 m at shallow depth (~1 km). The mechanism was reverse with a right lateral component (140º rake on the fault plane). This third rupture was equivalent to a M_w 5.7 event. The overall moment release for this model is equivalent to a M_w 6.9 earthquake. The model from the strong motion data underestimates the magnitude of the earthquake. The stations to the east of the rupture show some discrepancies in the waveform fit (Fig. 7), suggesting that more sources are involved in the rupture process. This is now the focus of joint research between seismologists and geodesists.

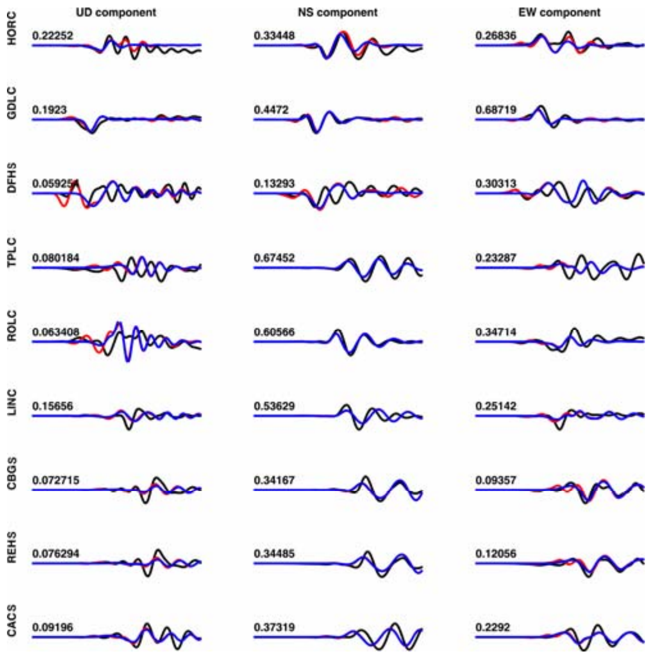

Figure 7. 3-component velocity seismograms (40 seconds) for the observed data (black), synthetic data from a single Greendale Fault rupture (blue), and for a joint 3-fault-plane model (red)

5 DISCUSSION: THE DARFIELD EARTHQUAKE, A COMPLEX RUPTURE SEQUENCE

All three proposed models agree that the Greendale Fault was the main source of the rupture sequence, but with the additional contribution of secondary blind fault sources. From the geodetic and strong motion data, we have been able to better define these blind faults as well as the likely rupture sequence: initiation of the rupture on a blind reverse fault just north of Greendale, followed by a major rupture of the Greendale Fault, triggering another rupture on a blind reverse fault west of Greendale. Dissipation of seismic energy in the gravels may account for the absence of clearly defined fault scarps despite the modelled predictions of near-surface fault slip for the Hororata and Charing Cross ruptures. All three models also agree that the rupture was complex at the eastern end of the Greendale Fault trace. Geological data show that the Greendale Fault trace steps over onto another east-west striking segment, but with different co-seismic deformation patterns than the main one. Geodetic and seismological data also show some discrepancies in the displacement/waveform fit of the data for the "eastern" GPS measurement points and strong motion stations. All source models also underestimate the overall magnitude of the earthquake, strongly suggesting that more blind sources are involved in the rupture process.

This work is a part of ongoing research on better defining the spatial extent and timing of the Darfield earthquake sequence and understanding the rupture mechanisms, which also includes detailed aftershock relocations and recently developed source tracking methods (Fry *et al.* 2011).

Acknowledgments: We would like to acknowledge our colleagues from GNS Science, GeoNet and University of Canterbury who participated in the collection and analysis of these datasets. Envisat data were provided by the European Space Agency (ESA) under the Cat-1 proposal AOALO3740. We have used ALOS data that is © Japan Aerospace Exploration Agency ("JAXA") and the Japanese Ministry of Economy, Trade and Industry ("METI") (2010). The data have been used with the permission of JAXA and METI and the Commonwealth of Australia (Geoscience Australia) ("the Commonwealth"). JAXA, METI and the Commonwealth have not evaluated the data as altered and incorporated in this paper, and therefore give no warranty regarding its accuracy, completeness, currency or suitability for any particular purpose. We would like to thank David Rhoades and Nicola Litchfield for the review of this paper.

REFERENCES:

Beavan, J., Samsonov, S., Motagh, M., Wallace, L., Ellis, S., Palmer, N. 2010. The M_w 7.1 Darfield (Canterbury) earthquake: geodetic observations and preliminary source model. *Bulletin of the New Zealand Society for Earthquake Engineering* 43(4): 228-235.

Di Carli, S., François-Holden C., Peyrat S., and Madariaga, R. 2010. Dynamic inversion of the 2000 Tottori earthquake based on elliptical subfault approximations, *J. Geophys. Res*., 115, B12328.

Cousins, J., McVerry, G., 2010, Overview of strong motion data from the Darfield Earthquake. *Bulletin of the New Zealand Society for Earthquake Engineering* 43(4). 222-227

Forsyth, P.J., Barrell, D.J.A., Jongens, R. 2008. Geology of the Christchurch area. Institute of Geological and Nuclear Sciences 1:250,000 Geological Map 16. 1 sheet +67 p. Lower Hutt, New Zealand. GNS Science.

Fry, B., Benites, R., Holden, C., Kao, H. Rupture scenarios for the M7.1 Darfield earthquake, 2011 Seism. Soc. Am. annual meeting, April 13-15, 2011. Memphis, USA

Gledhill, K., Ristau, J., Reyners, M., Fry, B., Holden, C. 2010. The Darfield (Canterbury) M_w 7.1 earthquake of September 2010: preliminary seismological report. *Bulletin of the New Zealand Society for Earthquake Engineering* 43(4): 215-221.

Gledhill, K., Ristau, J., Reyners, M., Fry, B., Holden, C. 2011. The Darfield (Canterbury, New Zealand) M_w 7.1 earthquake of September 2010: a preliminary seismological report. Submitted to *Seismological Research Letters*: in Press.

Quigley, M., Van Dissen, R., Villamor, P., Litchfield, N., Barrell, D., Furlong, K., Stahl, T., Duffy, B., Bilderback, E., Noble, D., Townsend, D., Begg, J., Jongens, R., Ries, W., Claridge, J., Klahn, A., Mackenzie, H., Smith, A., Hornblow, S., Nicol, R., Cox, S., Langridge, R., Pedley, K. 2010. Surface rupture of the Greendale Fault during the M_w 7.1 Darfield (Canterbury) earthquake, New Zealand: initial findings. *Bulletin of the New Zealand Society for Earthquake Engineering* 43(4): 236-242.

Stirling, M., Gerstenberger, M., Litchfield, N., McVerry, G., Smith, W., Pettinga, J., Barnes, P. 2008. “Seismic hazard of the Canterbury region, New Zealand: new earthquake source model and methodology”. *Bulletin of the New Zealand Society for Earthquake Engineering* 41: 51-67.

Van Dissen R. *et al*. 2011. Surface rupture displacement on the Greendale Fault during the Mw 7.1 Darfield (Canterbury) earthquake, New Zealand, and its impact on man-made structures, *in proceedings*, 9th Pacific Conference on Earthquake Engineering, NZSEE, Auckland, NZ: this volume.

Wells, D.L., Coppersmith, K.J. 1994. “New empirical relationships among magnitude, rupture length, rupture width, rupture area, and surface displacement”. *Bulletin of the Seismological Society of America* 84: 974-1002.

Wesnousky, S.G. 2008. “Displacement and geometrical characteristics of earthquake surface ruptures: issues and implications for seismic-hazard analysis and the process of earthquake rupture”. *Bulletin of the Seismological Society of America* 98: 1609-1632. doi: 10.1785/0120070111.

Zhao J., Uma S. R. 2011. A preliminary analysis on the response of an instrumented building during the 2010 Darfield earthquake - significant effects of soil structure interaction and nonlinear response, *in proceedings*, 9th Pacific Conference on Earthquake Engineering, NZSEE, Auckland, NZ: this volume.